Proceedings of Ninth World Conference on Earthquake Engineering
August 2-9, 1988, Tokyo-Kyoto, JAPAN (Vol.III)

4-3-2

IN-SITU MEASUREMENT OF PORE WATER PRESSURE DURING EARTHQUAKES

Eiji YANAGISAWA[1] and Hiroyuki OHMIYA[2]

[1] Department of Civil Engineering, Tohoku University, Sendai, Japan
[2] Civil Engineering Department, Tohoku Electric Power Inc. Sendai, Japan

SUMMARY

Seismic response of the ground and pore water pressure in sand layers including bed rock motion were obtained by an array observation system. Although the seismic intensity at the site was relatively small, definite zero offsets were seen in pore pressure records. The maximum of pore pressure has a strong relation to the maximum velocity at the ground surface. In order to simulate the pore pressure response in sand layers, one dimensional response analysis was carried out based on the anisotropic hardening model for saturated sand. It was found that the actual response of pore water pressure and distribution in the ground can be well approximated by the numerical model.

INTRODUCTION

There are sufficient numbers of laboratory tests on liquefaction of saturated sand during cyclic loading condition whereas very scarce studies are made on the actual behavior of pore water pressure in sand layers during earthquakes. Field measurement of pore pressure generated by an earthquake was made first by Uesawa et al in a soft organic soil layer below railway embankment during the Tokachioki-Earthquake of 1968 (Ref.1). Simultaneous measurement of seismic ground motion and pore pressure was made by Ikuta et al on the surface of basement wall of a building (Ref.2). Complete records of ground surface acceleration and pore pressure in free field condition were measured by Ishihara et al at Owi No.1 Island, Tokyo (Ref.3). During the earthquake sequence in Mammoth Lakes, Harp et al measured pore pressure and acceleration at the east shore of Convict Lake, California (Ref.4). They reported that despite the recording of acceleration as high as 148 gal none of pore pressure records show a clearly defined zero offset of excess pore pressure. The authors reported in the previous paper, however, that clear zero offsets were seen even in small amplitude of pore pressure response (Ref.5).

There has been published some papers so far on the field measurement of seismic induced pore pressure, but none of them describes characteristics of input waves nor bed rock motions, which seems to be essential for the response analysis of saturated sand layers with respect to pore pressure generation. This paper describes results of simultaneous measurement of pore pressure and seismic ground motion at a site, and some considerations were made on the vibrational characteristics of the ground motion. Then numerical analysis was made by solving governing equations of motion which describe interaction between porous solid and

pore fluid, where anisotropic hardening model was employed to simulate the actual undrained behavior of saturated sands.

INSTRUMENTATION AND SITE CHARACTERISTICS

Instrumentation for pore pressure measurement in sand layers was included in an array observation system named "KASSEM", which is composed of a center array and a strong ground motion array distributed in an area as shown in Fig.1. The center array system was constructed in Funaoka, Miyagi Prefecture and consists of a vertical array (V-series) and a horizontal array (H-series). As for the vertical array 6 three component seismometers of velocity type were equipped at the top of alluvium, diluvium, tuff and bed rock of granite, respectively. For the horizontal array observation points are distributed to form a equilateral triangle with the sides of 400m in the plane.

In surface sand layers piezometers with the capacities of 2kgf/cm^2 and 5kgf/cm^2 were also installed at the depth of 5m (P1), 13m (P2) and 16.5m (P3), respectively. The surface layer consists of strata of clay, silt, sand, silty sand and alternation of silt and sand layers, respectively. Fig.2 shows a soil boring log at an observation point of the center array. N-value of standard penetration test (SPT) and shear modulus obtained by velocity logging are shown in the same figure. The shear modulus which is estimated from the N-value and effective overburden pressure is also plotted in the figure. The estimated shear modulus coincides approximately with velocity logging results and laboratory test results for undisturbed samples obtained by resonant column method, which are designated by dots. Therefore the estimated values were used as the initial tangential modulus Go of layer elements.

RECORDED VELOCITY AND PORE PRESSURE

The observation began in September 1984, and several earthquake records including pore pressure response were obtained. An earthquake of January 9, 1987, of which the epicenter located at latitutde 39 51' 00"N, longitude 141 47' 00"E and depth 54km, was selected to the analysis. The magnitude of the earthquake was 6.6 in JMA scale and the seismic intensity at the site was around III in japanese scale. Velocity records obtained at the ground surface are shown in Fig.3. The maximum was 2.126, 3.201 and 0.929 kine for NS, EW and UD components, respectively. Pore pressure responses observed during the earthquake at three different depth were shown in Fig.4. Comparing the figure to the velocity record, it can be recognized that pore pressure increases suddenly when the principal motion begins. The magnitude of pore pressure rise becomes larger as the depth of piezometers increases, and clear zero offsets were seen, which indicates excess pore water pressure. The maximum of pore pressure was 46.7cm in head at P3 point. Fig.5 and 6 indicate Fourier spectra of velocity records and pore pressure records, respectively. Predominant period of velocity records are 1.00sec and 0.33sec for NS component, and 0.77sec and 0.33sec for EW component. Pore pressure records have high peaks in similar component except for longer period, which indicates the variation of excess pore water pressure.

According to the observation results the maximum of pore pressure has a strong relation to the maximum velocity observed at H1 point near ground surface. Fig.7 indicates maximum pore pressures observed at each point for six different earthquakes. The relation can be expressed by following equation:

$$U_{max} = 11.5(V_{max})^{1.23} \qquad (1)$$

The fact that pore pressure can be related to velocity seems to be reasonable, since velocity can be described by shear strain in the ground in every vibrational component. There must be a limiting value in the maximum pore pressure, which gives liquefaction state, where pore pressure reaches to the

overburden pressure. The coefficients of the equation are considered to be a function of material properties of sand, vibrational characteristics of the ground and stress state in the ground.

In order to see the relation between pore pressure and velocity, cross correlation function was calculated for first 4 seconds of the record and another 4 seconds of the principal motion. In the former case P-wave is considered to be predominant and in the latter case S-wave is predominant. Although values of cross correlation do not seem to be quite large, the periodicity can be clearly seen in both cases as shown in Fig.8. It should be noted that cross correlation between pore pressure and velocity is the largest among any other values such as displacement or acceleration. Considering the fact that P-wave arrives at the site prior to S-wave and at the beginning of the earthquake shorter period is predominant, primary stage of the response of pore pressure is due to P-wave. Comparing Fig.3 to 4, it is obviously recognized that excess pore pressure builds up as S-wave arrives at the site. The fact suggests the validity of fundamental assumptions for liquefaction analysis in which response to S-wave is primarily considered.

NUMERICAL RESPONSE ANALYSIS

In order to analyse the response of pore water pressure to earthquake excitations, one dimensional finite element analysis was carried out based on effective stress method. As for pore pressure generation there are some models to predict undrained behavior of sand during cyclic loading. In this paper anisotropic hardening model was employed to predict shear strain which results in volumetric strain which give rise to pore water pressure.

The equations governing the interaction of porous solid and liquid were first established by Biot and then the equations were extended to dynamic problems (Ref.6). Zienkiewicz et al applied these equations to nonlinear finite

$$\begin{bmatrix} M_s & 0 \\ 0 & M_s \end{bmatrix} \begin{Bmatrix} \ddot{U}_s \\ \ddot{U}_f \end{Bmatrix} + \begin{bmatrix} C_1 + \mathring{K}_1 & -C_2 + \mathring{K}_2 \\ -C_2 + \mathring{K}_2 & C_2 + \mathring{K}_3 \end{bmatrix} \begin{Bmatrix} \dot{U}_s \\ \dot{U}_f \end{Bmatrix} + \begin{bmatrix} K & 0 \\ 0 & 0 \end{bmatrix} \begin{Bmatrix} U_s \\ U_f \end{Bmatrix} = \begin{Bmatrix} f_s \\ f_f \end{Bmatrix} \qquad (2)$$

where M; mass matrix C, $\mathring{K}$; viscous matrix K; stiffness matrix
U; absolute displacement (vertical and horizontal components)
Subscripts s and f indicate the components for solid and liquid, respectively. Pore pressure can be introduced from compatibility equations and defined as

$$p = \rho_f \, g \, \mu \, [(1-n)U_{i,i} + n \, U_{i,i}] \qquad (3)$$

where n;porosity g;the gravity acceleration ρ_f;the density of water.
μ is a parameter introduced to approximate in compressibility of fluid. In the analysis is assumed to be 10^{11}. Direct integration of Eq.(2) was made by Newmark's method assuming β=0.3025 and γ=0.6.

One dimensional response analysis was performed on the site, in which the surface layers were divided into 26 elements as shown in Fig.2. Horizontal component of H2 motion perpendicular to the direction to the epicenter was regarded as input motion. Fig.9 indicates calculated response of the ground and observed one at H1 point. Although the calculation seems to give slightly smaller response than observed one, characteristics of waves are considerably well approximated by the model. A typical example of hysteretic loop of an element No.9 near P2 point was shown in Fig.10, which does not necessarily indicate definite nonlinearity in stress strain relationship, because the input waves was relatively small to cause liquefaction. Considering magnitude of the earthquake and the intensity at the site, this tendency would be reasonable.

Fig.11 indicates pore pressure distribution in the ground calculated in this analysis. Measured values are also plotted in the same figure. Pore pressure in the shallow part of the ground increases rapidly as time passes, and in the deeper part of the surface layer pore pressure increases remarkablely after a while. Time histories of pore pressure calculated at each observation point are

shown in Fig.12 together with measured values, which has been smoothed by digital filter to extract excess pore pressure. The accuracy of calculation is almost satisfactory. Although the analysis was simple, the response of the ground including pore pressure was well approximated by this model.

CONCLUSIONS

Response of soft surface layers and pore pressure in sand layers during earthquakes was simultaneously measured by an array observation system. The seismic records contain bed rock motion at the depth of 406m, therefore input waves to surface layer can be apparently derived from observed velocity records. It is found from the observation that the maximum of pore pressure response has close relation to the maximum velocity at the ground surface, which can be described by an empirical equation. Although intensity of the earthquake was relatively small, definite zero offsets were seen in the excess pore pressure by 14.2cm in head at P3 point.

Then one dimensional finite element response ananlysis was carried out for surface layers in order to investigate the pore pressure behavior at the site. By use of effective stress model based on the anisotropic hardening theory it is found that excess pore pressure generated during earthquake can be well approximated.

ACKNOWLEDGMENT

The authors wish to express their sincere appreciation to Dr. Teruo Shimizu of Kumagaigumi Co. Ltd. and Prof. Makoto Kamiyama of Tohoku Institute of Technology for their kind assistance to the array observation.This study is partly subsidized by the Grant-in-aid of the Ministry of Education of the Japanese Government.

REFERENCES

1. Uesawa,H. and Kumagai J., Measurement of Pore water pressure during Tokachi-Oki Earthquake," 4th Annual Meeting of JSSMFE, 39-42, (1969)
2. Ikuta, K., Maruoka, M. Mitoma, T. and Nagano M. "Record of Lateral Pressure Taken during Earthquake," Soils and Foundations, Vol.19 No.4, 89-92 (1979)
3. Ishihara, K., Shimizu, K. and Yamada Y., "Pore Water Pressure Measured in Sand Deposits during An Earthquake, Soils and Foundations, Vol.21 No.4, 85-100, (1981)
4. Harp, E.L., Sarmiento, J. and Cranswick E., "Seismic-induced Pore Water Pressure Records from The Mammoth Lakes,California, Earthquake Sequence of 15 to 17 May 1980," Bull. Seism. Soc. Am. Vol.74, 1381-1393, (1984)
5. Yanagisawa E. and Ohmiya H., "Seismic Response of Pore Water Pressure in Surface Sand Layers," Soil Dynamics and Liquefaction, 221-229, Elsevier, (1987)
6. Biot M. A., "Generalized Theory of Acoustic Propagation in Porous Dissipative Media," J. Acoust. Soc. of America, Vol.34 No.9, 1254-1264, (1962)
7. Zienkiewicz, O. C. and Shiomi T., "Dynamic Behavior of Saturated Porous Media," ;The Generalized Biot Formulation and Its Numerical Solution," Intn. J. Numer. and Analy. Meth. in Geomechanics, Vol.8, 71-96, (1984)

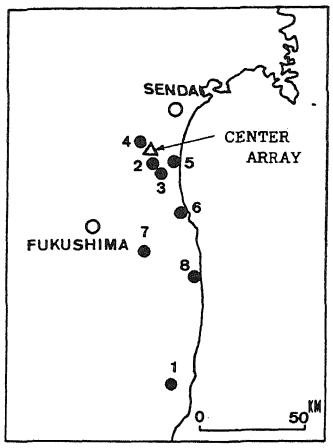

Fig.1 Location of the site

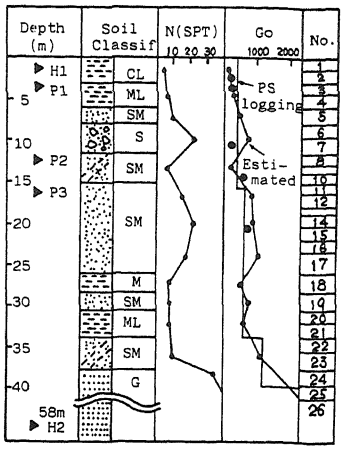

Fig.2 Soil profile at the site

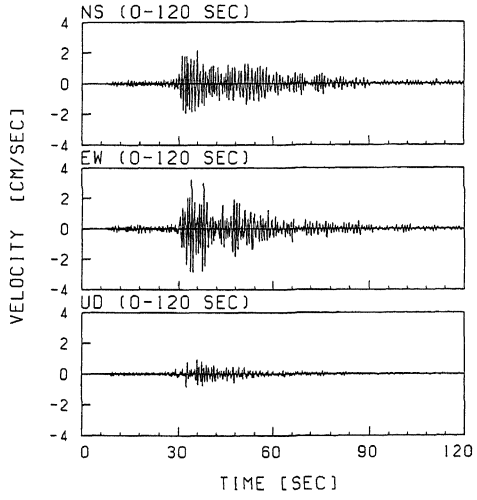

Fig.3 Velocity record at H1

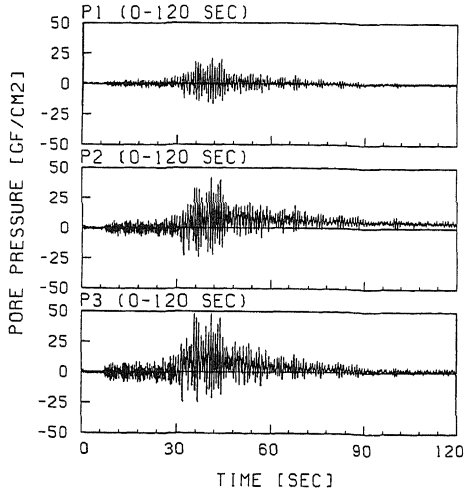

Fig.4 Pore pressure record

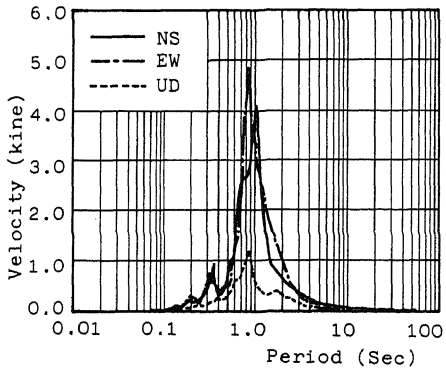

Fig.5 Fourie spectrum of velocity

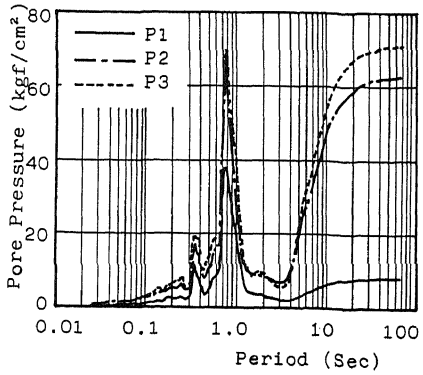

Fig.6 Fourier spectrum of pore water pressure

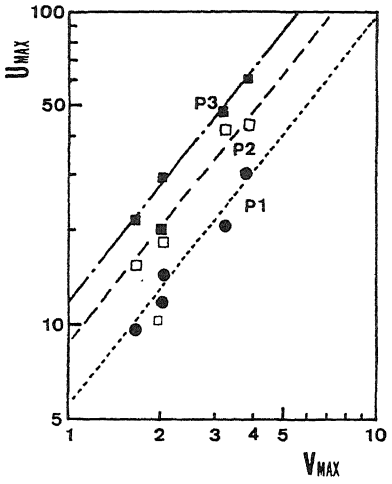

Fig.7 Relation between Umax and Vmax

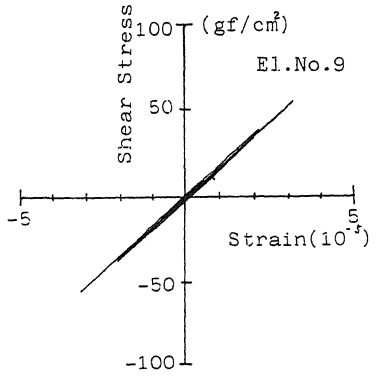

Fig.10 Hysteretic loop

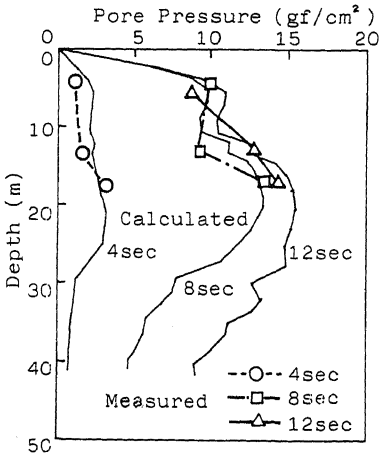

Fig.11 Pore pressure distribution

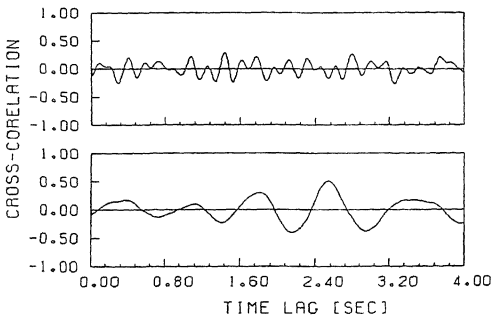

Fig.8 Cross-correlation function

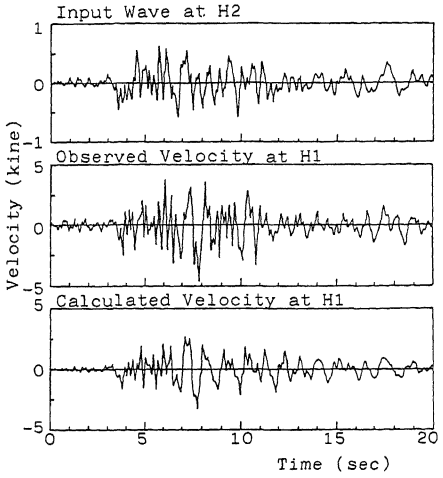

Fig.9 Response of the ground

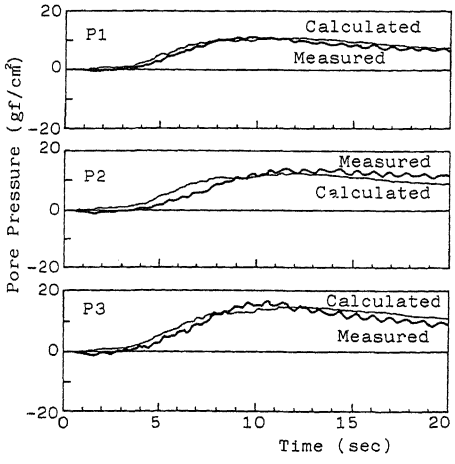

Fig.12 Response of pore pressure